**Rare Metal Materials and Engineering**
Volume 52, Issue 4, April 2023
Available online at www.rmme.ac.cn

Science Press

**Cite this article as**: Bi Guangli, Qi Jiachen, Jiang Jing, et al. Wetting of MgO, $TiO_2$ and Stainless Steel by Molten Al-8Si Binary Alloy at 1173 K[J]. Rare Metal Materials and Engineering, 2023, 52(04): 1251-1258.

ARTICLE

# Wetting of MgO, $TiO_2$ and Stainless Steel by Molten Al-8Si Binary Alloy at 1173 K

**Bi Guangli[1,2], Qi Jiachen[1,2], Jiang Jing[1,2], Lin Qiaoli[1,2], Li Yuandong[1,2], Chen Tijun[1,2], Ma Ying[1,2], Guan Renguo[3]**

*[1] State Key Laboratory of Advanced Processing and Recycling of Nonferrous Metals, Lanzhou University of Technology, Lanzhou 730050, China; [2] School of Material Science and Engineering, Lanzhou University of Technology, Lanzhou 730050, China; [3] School of Materials Science and Engineering, Dalian Jiaotong University, Dalian 116028, China*

**Abstract:** The wettability and interface microstructures of Al-8Si/stainless steel, Al-8Si/MgO, and Al-8Si/$TiO_2$ systems were investigated by a modified sessile drop method. The formation of interface products of three systems was discussed from the view of thermodynamics. Results show that the interface microstructure of Al-8Si/stainless steel is composed of $Fe(Al,Si)_3$, $Al_{7.2}Fe_{1.8}Si$ and $Fe_2Al_5$ phases, while that of Al-8Si/MgO and Al-8Si/$TiO_2$ systems consists mainly of the $Al_2O_3$ phase with different morphologies and roughness. The wettability results indicate that the Al-8Si/MgO system exhibits a better non-wettability compared with the stainless steel and $TiO_2$ substrates, whose equilibrium wetting angle is 124°. The wettability differences of the three systems are mainly related to the roughness and properties of interface products. The interface roughness tests show that the interface of Al-8Si/MgO system has the largest roughness of 1.46 μm, which is mainly due to the evaporation of Mg that destroys the morphology of the interface reaction layer during the interface reaction process. Furthermore, the existence of Ti promotes the interface reaction and increases the thickness of interface reaction layer and thus reduces the equilibrium wetting angle of Al-8Si/$TiO_2$ system.

**Key words:** Al-8Si alloy; wettability; 2520 stainless steel; $TiO_2$; MgO

Recently, Al-Si alloys have been widely used in communication industries owing to their high tensile strengths and toughness, good thermal conductivity, and ease of precision machining. Inclined plate casting, a novel semi-solid rheological slurry preparation technology, can be used to efficiently fabricate Al alloy thin-walled parts with complex size in combination with die casting, especially for the filters of 5G base station[1]. However, the adhesive problem between Al-Si alloy melts and the inclined plate (stainless steel) is difficult to solve when the semi-solid slurry passes through the inclined plate in practical production (Fig. 1). This will directly affect the quality and efficiency of semi-solid slurry preparation.

It is reported that some ceramic coatings prepared on stainless steel plate can markedly reduce the adhesive phenomenon through the non-wettability between Al melts and ceramics, such as $ZrO_2$[2], MgO[3], ZnO[4], SiC[5], $Al_2O_3$[6] and $TiO_2$[7]. Aside from structure, physical and chemical properties, atmosphere environment (Ar or vacuum), roughness, interfacial reaction products, substrate type (active or inactive metals), and measurement techniques also influence the wettability of ceramics. Generally, the interfacial wetting is mainly characterized by the equilibrium contact angle ($\theta$) according to Young's equation:

$$\cos\theta = \frac{\sigma_{sv} - \sigma_{sl}}{\sigma_{lv}} \tag{1}$$

where $\sigma_{sv}$, $\sigma_{sl}$ and $\sigma_{lv}$ are the solid-vapor, solid-liquid and liquid-vapor interfacial tensions, respectively. Wetting of a solid surface by a liquid is achieved when $\theta<90°$; otherwise, it is non-wetting ($\theta>90°$)[8]. Ueki et al[2] investigated the wettability of different Al melts and $ZrO_2$, and pointed out that Al melts are non-wettable with $ZrO_2$, whose $\theta$ value is about 145° at 1173 K. Also, Yang's experimental results suggest that the $\theta$ value is 148° at 973 K for the Al melts and $ZrO_2$ substrate due

Received date: June 16, 2022
Foundation item: National Key Research and Development Program (2018YFB2001800); National Natural Science Foundation of China (51961021, 52001152); Undergraduate Innovation and Entrepreneurship Training Program (DC2021011, DC2021018, DC2021036)
Corresponding author: Bi Guangli, Ph. D., Professor, State Key Laboratory of Advanced Processing and Recycling of Nonferrous Metals, Lanzhou University of Technology, Lanzhou 730050, P. R. China, Tel: 0086-931-2976378, E-mail: glbi@163.com

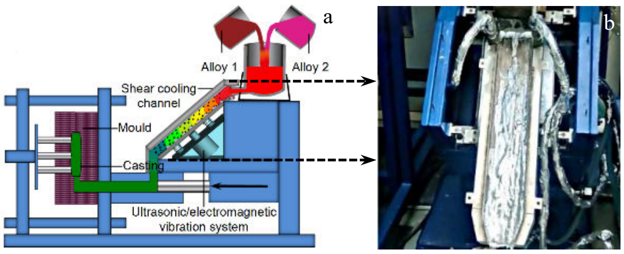


Fig.1 Schematic diagram of semi-solid metal slurry prepared by shear/vibration coupling and rheological casting (a) and typical Al-8Si alloy metals slurry remained on the inclined plate after casting (b)

to the existence of the oxide film of Al melts[9]. Additionally, Shen et al[3] reported the wettability of Al melts and single crystal MgO with three different faces of (100), (110) and (111) at 1073 – 1473 K in an Ar-3%$H_2$ atmosphere. The experimental results indicate that the wettability of Al melts neither depends on the substrate orientation nor on the temperature. The $\theta$ value of the Al/MgO system is possibly between 90° and 105° under the aforementioned conditions owing to the formation of $\alpha$-$Al_2O_3$ reaction products. The larger $\theta$ value (100°–107°) is also obtained at the interface between Al melts and single crystal ZnO with various orientations after 5 – 20 min at 1273 K, which is mainly attributed to the non-wetting reaction products of $\alpha$-$Al_2O_3$[4]. An et al[10] demonstrated that the initial contact angle of the Al melts and SiC is 154° at 1173 K, arising from the presence of oxide film on the Al melt surface, which decreases to 54° at equilibrium as a result of the $Al_4C_3$ reaction product. Avraham et al[11] studied that the effects of temperature (973–1273 K) on the wettability of Al melts and $TiO_2$, and proposed that the system has a good non-wettability at 973 K with the $\theta$ of ~150° due to low temperature and non-reactivity at the solid-liquid interface.

As mentioned above, the wetting of ceramics by molten pure aluminum was extensively studied[2–11]. However, the wettability of ceramics by molten Al-Si alloys was seldom reported. Therefore, in this study, the wetting of three substrates (stainless steel, $TiO_2$ and MgO) with Al-8Si melts was investigated at 1173 K using a modified sessile drop method.

## 1 Experiment

### 1.1 Material preparation

The stainless steel (2520), MgO, and $TiO_2$ polycrystalline ceramics (substrate material) were machined into the samples with a size of 30 mm×30 mm×6 mm and polished to a surface roughness of 1 – 2 μm. The experimental Al-8Si alloy (deposition material on stainless steel and ceramics) was used to observe the wetting and spreading behavior, which was prepared with pure Al (99.999%) and Al-30%Si master alloy in a graphite crucible put on an electric resistance furnace at 973 K. The melt was stirred and kept at 953 K for 20 min and poured into the preheated cylindrical iron mold at 473 K. The mould was 150 mm in height and 50 mm in diameter. The substrates and Al-8Si alloy were ultrasonically cleaned before placed in the chamber.

### 1.2 Wetting test

A wetting test was carried out on a sessile drop equipment that contained a high vacuum system, tube furnace, data acquisition and processing system and drop shape analysis software in the computer terminal, and the details can be referred in Ref.[12–13]. Al-8Si alloy sample with a mass of 0.03 g was firstly heated to 573 K at 15 K/min, and then heated to 1173 K at 20 K/min after holding for 10 min in a vacuum of $7\times10^{-4}$ Pa. When the temperature remained stable under a vacuum of $5\times10^{-4}$ Pa, the alloy sample was directly dropped through an open alumina tube and deposited on three substrates. The variation of the whole wetting process was recorded by an infrared camera at 15 s intervals. The contact angle and drop base radius of all samples were analyzed from the profiles using Surface Meter Elements Analysis software. When the wetting experiments ended, the whole chamber was cooled under a flowing Ar (~99.999%) atmosphere at a rate of 15 K/min to the room temperature.

### 1.3 Interface microstructure characterization

The morphology, composition, and interface microstructure of a cross-section of Al-8Si/MgO, Al-8Si/$TiO_2$ and Al-8Si/stainless steel systems were characterized by optical microscopy (OM, LSM800) and scanning electron microscopy (SEM, Quanta Feg 450) equipped with an energy dispersing spectrometer (EDS). For SEM observation, all samples were roughly and finely ground with 400#, 600#, 800# and 1000# sandpapers and mechanically polished, and then etched for ~30 s in Keller's reagent for 13 s for corrosion. The samples were immersed into a NaOH aqueous solution to remove the solidified Al-8Si alloy for the subsequent roughness analysis. The roughness of three substrates was measured by confocal laser scanning microscope (CLSM).

## 2 Results and Discussion

### 2.1 Wetting behavior

Fig.2a shows the variation of the contact angle ($\theta$) of Al-8Si alloy melts on stainless steel, MgO, and $TiO_2$ with time at 1173 K. It can be seen that the $\theta$ value of MgO and $TiO_2$ substrates slowly decreases, but that of stainless steel substrates rapidly drops at less than 500 s. Conversely, the contact angle of three substrates is close to a constant value, that is, the equilibrium contact angle (ECA) at 30 min. The initial contact angle of the Al-8Si alloy melts on MgO, $TiO_2$ and stainless steel is similar, i.e. 143°, 144° and 137°, respectively. The presence of the oxide film on Al-8Si alloy melts leads to a high initial contact angle. The process of eliminating the oxide film on the surface of the alloy melts is accompanied by the formation of vapor-phase $AlO_2$ and interface products, which improve the wettability of the interface. The corresponding reaction equation at the interface of the melts is follows:

$$Al_2O_3 + Al(l) \rightarrow Al_2O(g) \quad (2)$$

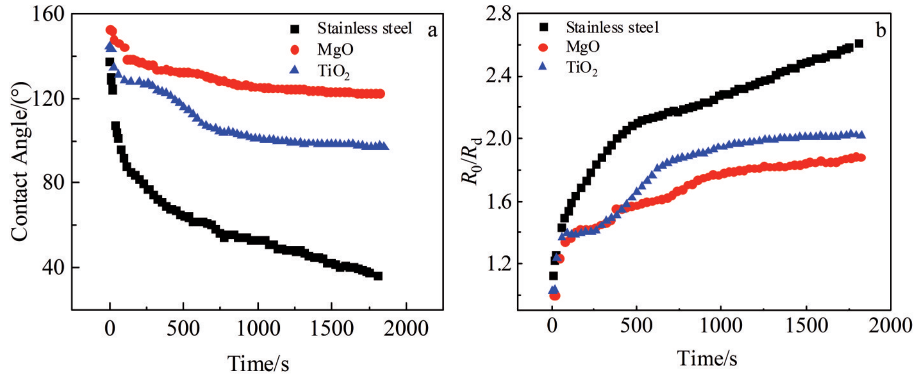


Fig.2 Variations of contact angle (a) and normalized contact radius $R_0/R_d$ (b) with time for Al-8Si alloy melts on MgO, $TiO_2$, and stainless steel at 1173 K

When the interface starts to react, the equilibrium contact angle depends on the characteristics of the reaction product. As shown in Fig.3, at higher temperatures (1173 K), the liquid drops of three systems show different spreading behavior, and the final equilibrium contact angles reach 29° (stainless steel), 96° ($TiO_2$) and 124° (MgO). This trend can be reflected by the variation of normalized contact radius of Al-8Si alloy melts on three substrates with time at 1173 K, as shown in Fig.2b.

## 2.2 Interfacial microstructures

SEM images and EDS mappings of interface reaction layer of Al-8Si alloy melts on stainless steel are shown in Fig. 4. According to EDS results (Table 1), the interface reaction products of Al-8Si/stainless steel are primarily composed of $Fe(Al,Si)_3$, $Al_{7.2}Fe_{1.8}Si$ and $Fe_2Al_5$ phase, as reported by Liu et al[14]. It is known that Al-8Si/stainless steel is a typical reactive wetting system which inevitably leads to the formation of intermetallic compounds. Actually, the formation order of these interface products determines the distribution of the reaction layer. It can be calculated that the interfacial free energy ($\Delta G^0$) of $Fe(Al,Si)_3$, $Al_{7.2}Fe_{1.8}Si$ and $Fe_2Al_5$ are −83.4, −184.4 and −138.4 kJ/mol at 1173 K, respectively, according to the following equations:

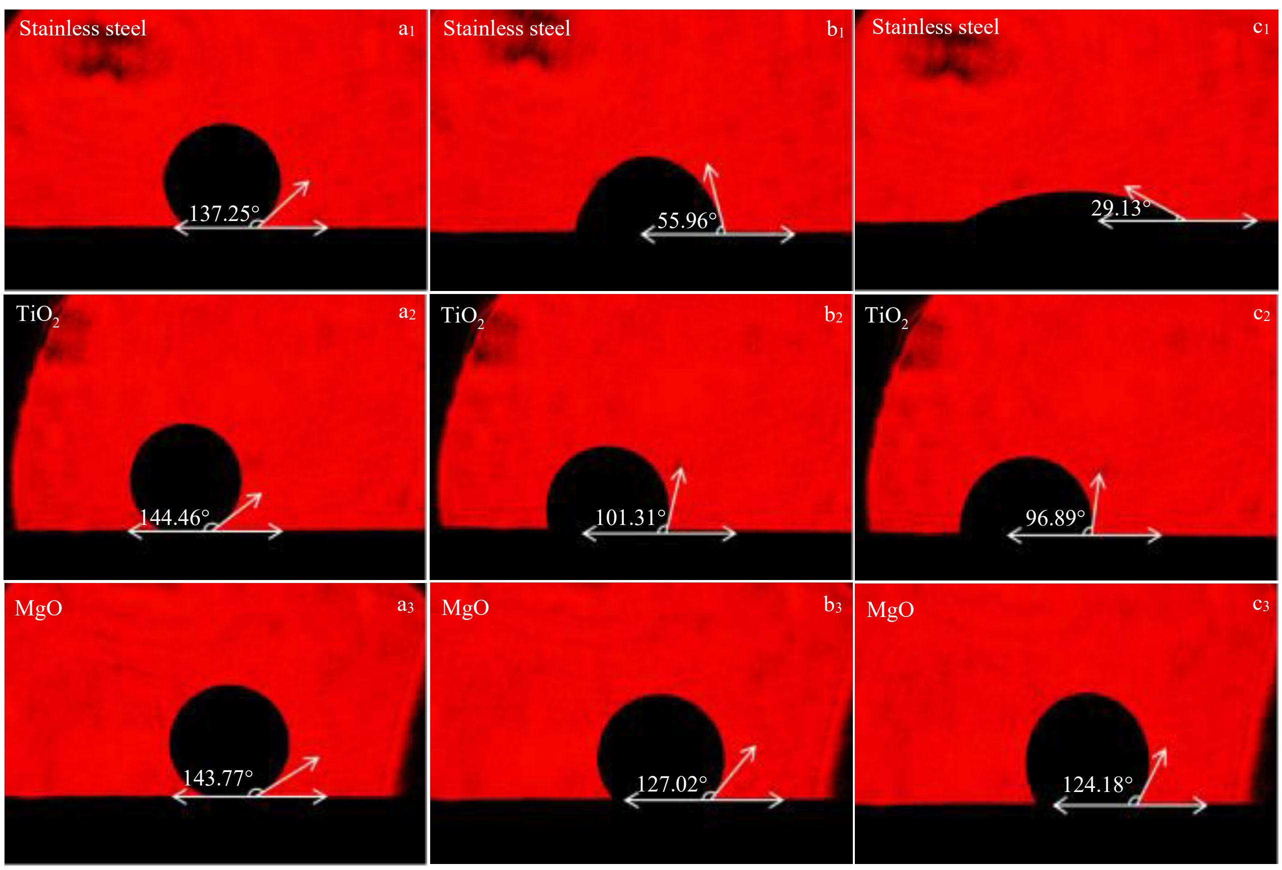


Fig.3 Contact angles of Al-8Si alloy melts on stainless steel, $TiO_2$ and MgO at 0 s ($a_1$–$a_3$), 900 s ($b_1$–$b_3$), and 1800 s ($c_1$–$c_3$)

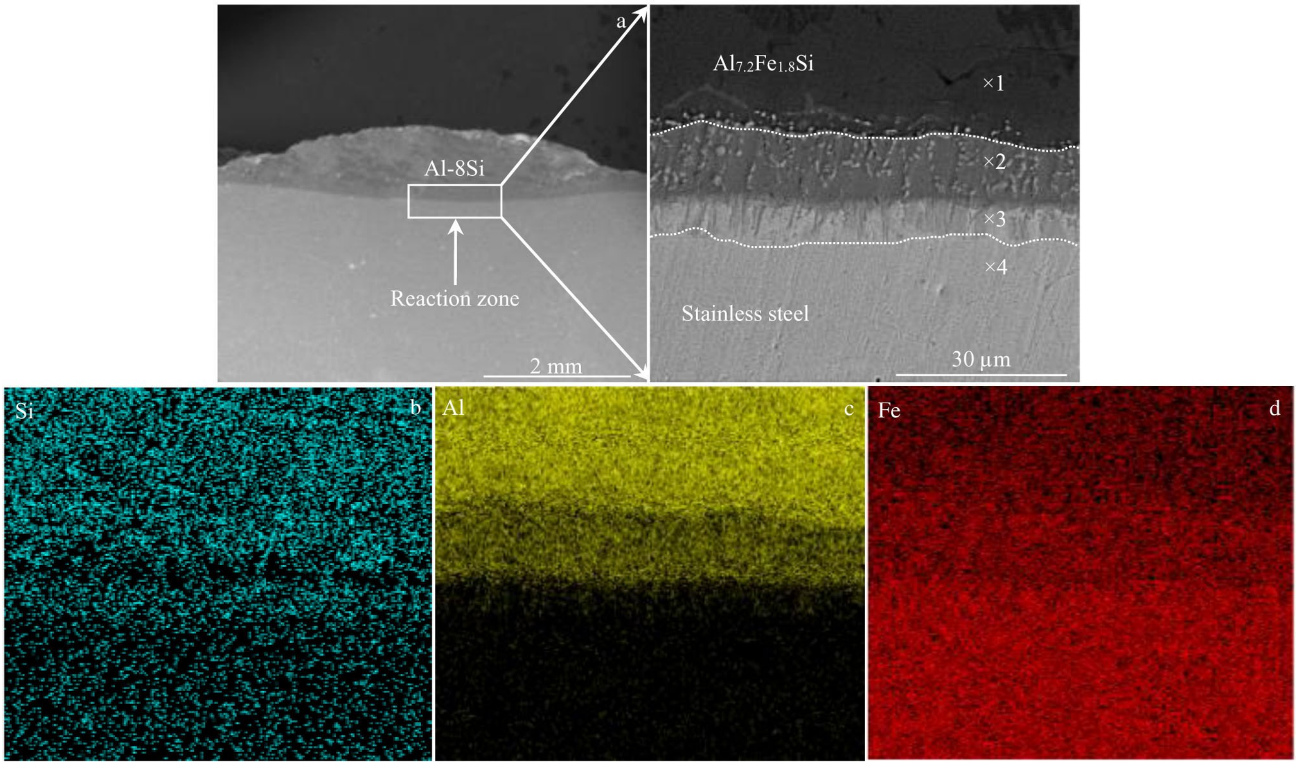


Fig.4 SEM images (a) and EDS mappings of element Si (b), Al (c), and Fe (d) at interface of Al-8Si/stainless steel

$$\Delta G^0_{FeAl_3} = -142770 + 50.58T \quad (3)$$

$$\Delta G^0_{Fe_2Al_5} = -253971 + 98.52T \quad (4)$$

$$\Delta G^0_{Al_{7.2}Fe_{1.8}Si} = -295355 + 94.59T \quad (5)$$

It can be seen that the $\Delta G^0$ value of $Al_{7.2}Fe_{1.8}Si$ phase is more negative than that of other phases, which indicates that the phase should precipitate preferentially at the interface of Al-8Si/stainless steel. The similar interface microstructure was also reported for Al alloy/stainless steel joint prepared by tungsten inert gas welding-brazing[15].

The interface microstructure and EDS mappings of the Al-8Si/$TiO_2$ is displayed in Fig. 5. The smooth surface reaction layer is observed at the interface, as seen in Fig. 5a. EDS results in Table 2 indicate that the interface reaction products are mainly composed of $Al_2O_3$ phase that contains a small amount of Ti. It is reported that the interface reaction of the Al/$TiO_2$ system is relatively complex at high temperatures[7]. Generally, three reactions will occur at the Al/$TiO_2$ interface as follows:

$$4Al + 3O_2 \rightarrow 2Al_2O_3 \text{ (Al surface oxidation)} \quad (6)$$

$$4Al + Al_2O_3 \rightarrow 3Al_2O \text{ (Al surface deoxidation)} \quad (7)$$

$$Al + TiO_2 \rightarrow Al_2O_3 + TiO_{2-x} \quad (8)$$

**Table 1 EDS results of each point marked in Fig.4a (at%)**

| Point | Al | Fe | Si | Cr | Ni | Phase |
|---|---|---|---|---|---|---|
| 1 | 68.6 | 13.8 | 7.3 | 8.6 | 1.6 | $Al_{7.2}Fe_{1.8}Si$ |
| 2 | 59.1 | 20.3 | 5.8 | 10.0 | 4.7 | $Fe(Al,Si)_3$ |
| 3 | 43.4 | 26.1 | 6.7 | 12.5 | 11.4 | $Fe_2Al_5$ |
| 4 | 0.6 | 52.0 | 1.6 | 28.4 | 17.3 | $\alpha$-Fe |

$$Al + TiO_2 \rightarrow Al_2O_3 + [Ti]_{Al} \quad (9)$$

At 1173 K[16], the value of Gibbs free energy for $Al_2O_3$ (−1295.046 kJ/mol) is lower than that of $Al_2O$ (−231.473 kJ/mol), AlTi (−64.378 kJ/mol), TiO (−427.976 kJ/mol) and $AlTi_3$ (−108.491 kJ/mol), and thus the $Al_2O_3$ phase is easier to form at the interface. Avraham et al[11] also confirmed that the interface reaction product of Al/$TiO_2$ is mainly $Al_2O_3$ at 1273 K. Fig. 6 shows SEM images and EDS mappings of reaction layer at Al-8Si/MgO interface. The reaction product is $Al_2O_3$ with a rough morphology based on the EDS results in Table 3. Due to different experimental conditions, there are two kinds of interface reaction products for the Al/MgO system at present. One is $Al_2O_3$[3] and the other one is $MgAl_2O_4$[17]. Actually, $MgAl_2O_4$ is easy to form at high interface reaction temperatures (>1300 K), which will further hinder the oxidation of Al. In the present work, only $Al_2O_3$ is generated at low interface reaction temperature (1173 K), and the corresponding interface reaction is following[18]:

$$2Al + 3MgO \rightarrow Al_2O_3 + 3Mg\uparrow \quad (10)$$

### 2.3 Discussion

The wettability of substrate is mainly related to the interfacial properties. Among the factors determining wettability, the interfacial reaction product is not negligible[19–21]. In our work, different interface products between Al-8Si melts and substrates during reaction determine various wetting properties. When the interface products are the same, the roughness of the interface products and the active elements affect the wettability.

In the Al-8Si/stainless steel system, the loose interfacial

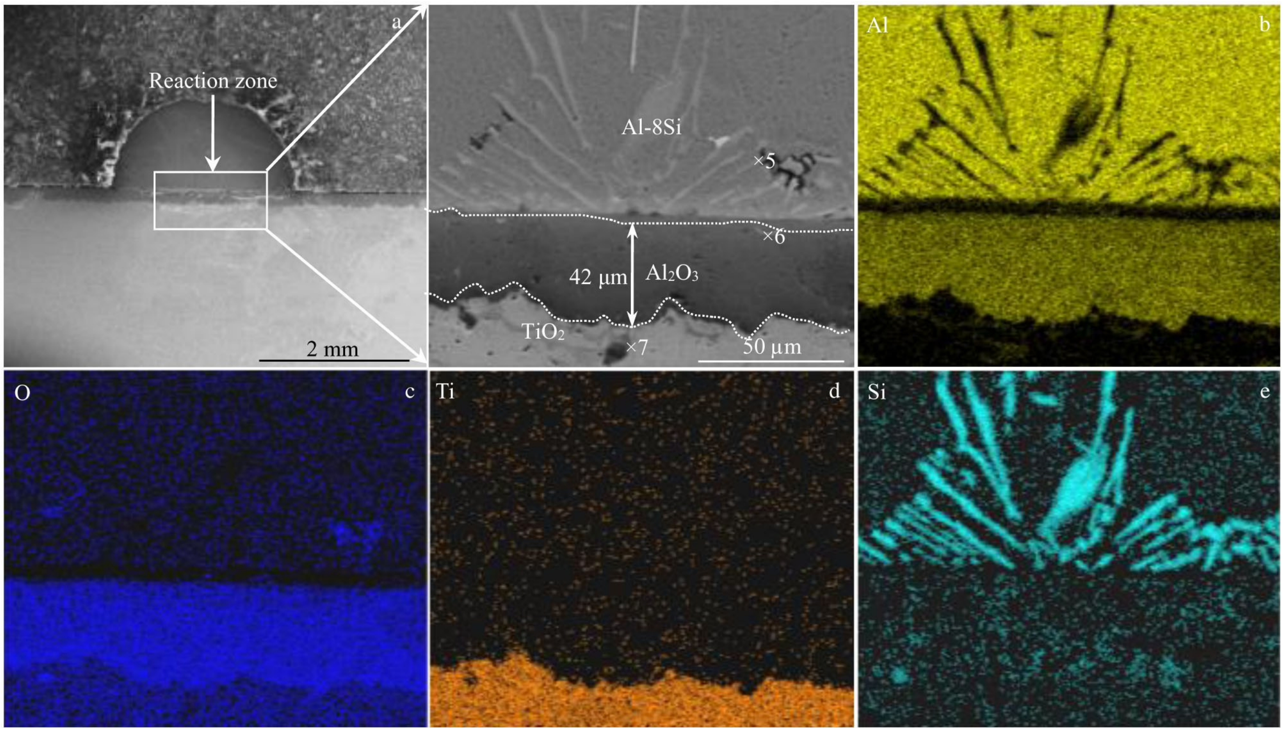


Fig.5 SEM images (a) and EDS mappings of element Al (b), O (c), Ti (d), and Si (e) at interface of Al-8Si/$TiO_2$

**Table 2 EDS results of each point marked in Fig.5a (at%)**

| Point | Al | Si | O | Ti | Phase |
|---|---|---|---|---|---|
| 5 | 84.06 | 11.73 | 3.84 | 0.39 | $\alpha$-Al |
| 6 | 41.09 | 0.29 | 57.78 | 0.84 | $Al_2O_3$ |
| 7 | 1.97 | 0.1 | 61.25 | 36.68 | $TiO_2$ |

reaction layer consists of $Al_{7.2}Fe_{1.8}Si$, $Fe(Al, Si)_3$ and $Fe_2Al_5$ phase at the interface (Fig.4). It is obvious that these reaction products tend to grow simultaneously inside the droplet and substrate, and form a dissolution-diffusion channel at the interface owing to the large solid solubility of Fe in Al-Si melts. So, the diffusion of Fe and other elements in the triple phase line is enhanced, which also promotes the extension of triple phase line region and finally improves the wetting properties of Al-8Si/stainless steel system[22].

Compared with Al-8Si/stainless steel, the dense $Al_2O_3$ reaction layer forms at the interface of the Al-8Si/MgO and

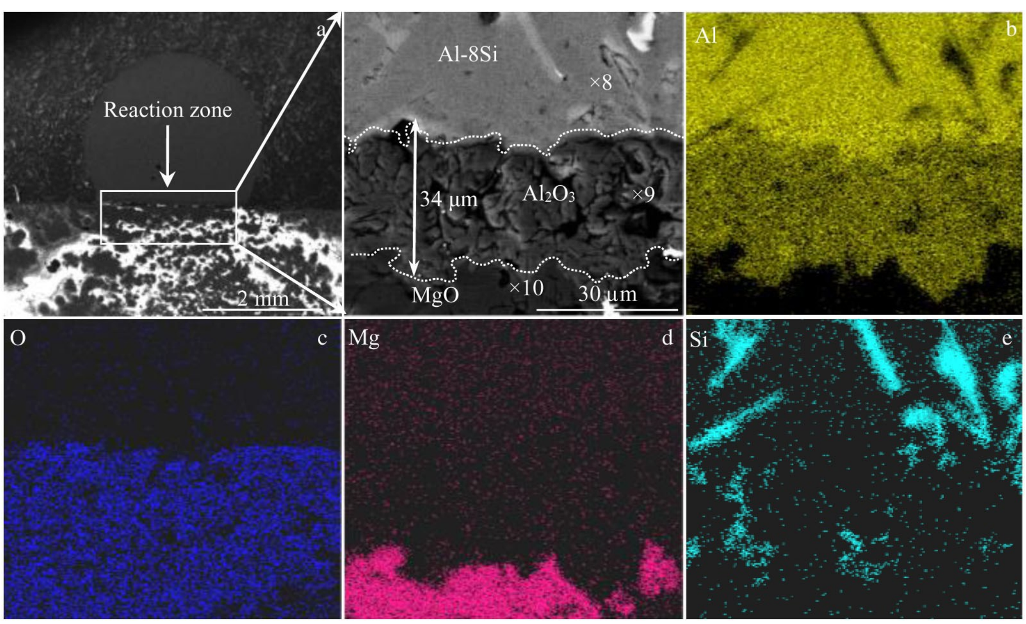


Fig.6 SEM images (a) and EDS mappings of element Al (b) O (c), Mg (d), and Si (e) at interface of Al-8Si/MgO

**Table 3 EDS results of each point marked in Fig.6a (at%)**

| Point | Al | Si | O | Mg | Phase |
|---|---|---|---|---|---|
| 8 | 89.8 | 3.4 | 6.7 | 0 | $\alpha$-Al |
| 9 | 60.4 | 0.2 | 39.4 | 0 | $Al_2O_3$ |
| 10 | 0.3 | 0 | 46.2 | 53.5 | MgO |

Al-8Si/$TiO_2$ systems, which prevents the atomic diffusion in the triple phase line and results in a large equilibrium contact angle. Although interface products $Al_2O_3$ appears at the interface of both systems, their roughness is different, which is the main factor affecting wetting properties of Al-8Si/MgO and Al-8Si/$TiO_2$ system. For example, Qi et al[23] found that the average contact angle is significantly increased by 16.4° when $R_a$ value increases from 0.092 μm to 0.834 μm for Pb/$Al_2O_3$ system at 973 K. So, it can be seen that the surface roughness of the interface is one of the key factors affecting the wettability of $Al_2O_3$. Fig. 7 shows the roughness of interface products of Al-8Si/stainless steel, Al-8Si/MgO and Al-8Si/$TiO_2$ systems. It can be found that the interface roughness (1.46 μm) of Al-8Si/MgO system is an order of magnitude higher than that of Al-8Si/stainless steel (0.573 μm) and Al-8Si/$TiO_2$ (0.528 μm). The large interface roughness of Al-8Si/MgO mainly arises from the formation of loose macro-pores due to the evaporation of Mg during the interface reaction (Fig. 6). It should be emphasized that the roughness is proportional to the surface area of the interface reaction layer. This relationship can be reflected by a schematic diagram in Fig. 8, which indicates the variation of surface area with smooth or rough interface. Furthermore, the surface free energy ($G$) and surface area ($A$) satisfy the following linear relation:

$$dG = \sigma dA \tag{11}$$

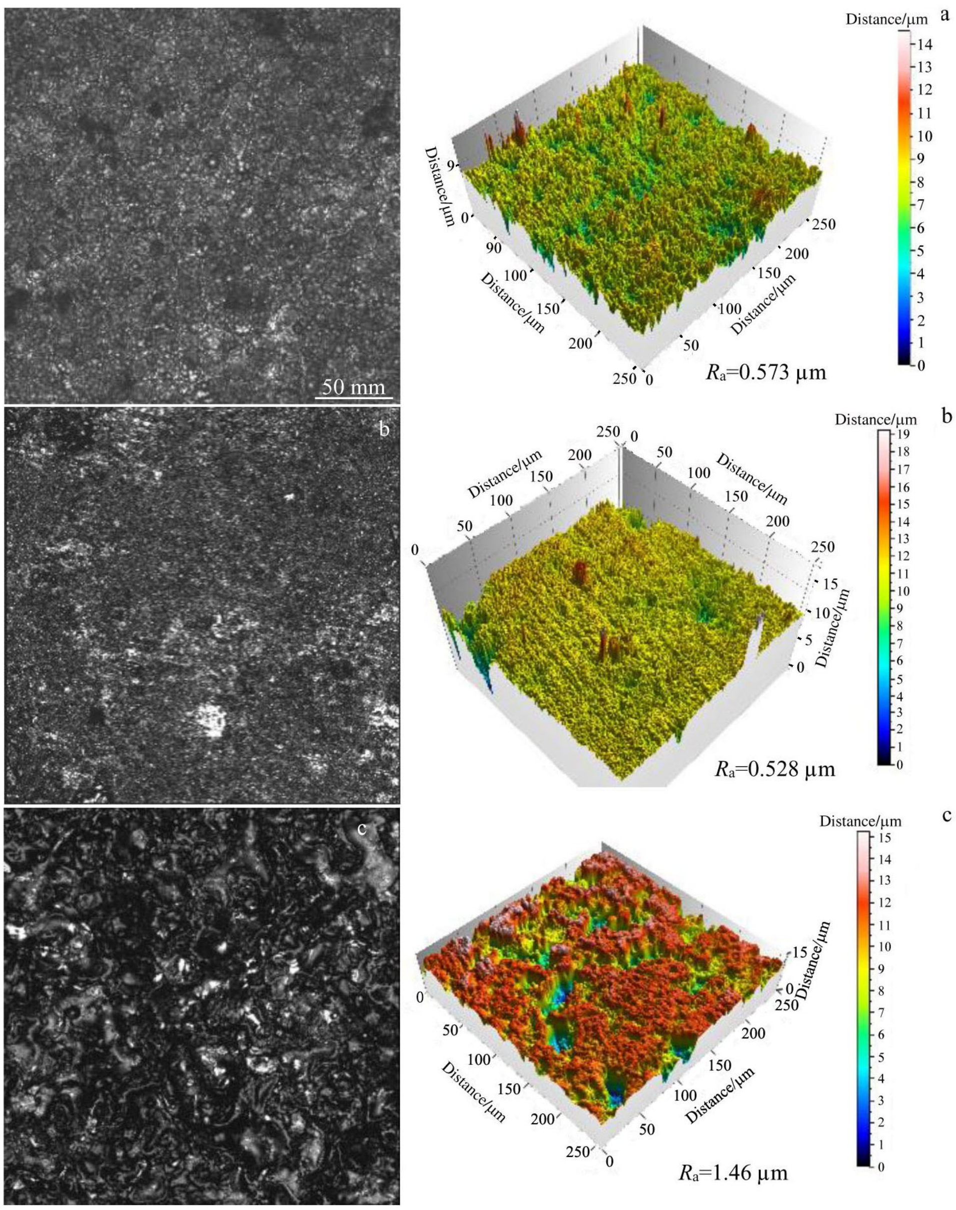


Fig.7 CLSM images of 2520 stainless steel (a), $TiO_2$ (b), and MgO (c) substrate surface

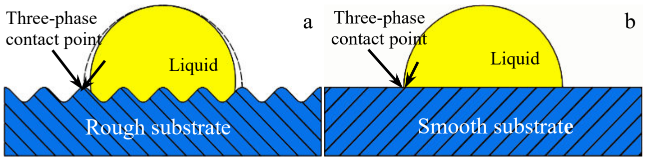


Fig.8 Schematic diagrams showing the wetting of liquid on rough (a) and smooth (b) substrates

where $\sigma$ is a constant. Accordingly, it can be concluded that the large interface roughness directly leads to an increase in surface free energy ($\gamma_{sv}$) of interface reaction layer. Based on the modifier formula of Berthelot rule[24], the $\gamma_{sv}$ values of each system can be calculated through Eq. (12) using equilibrium wetting angle ($\theta$), where $\theta$ is the contact angle for the Al-8Si/ceramic system, and $\beta$ is the constant ($\beta$=1.247× $10^{-4}$ m²/mJ), $\gamma_{lv}$ is the surface free energy of the Al-8Si alloy melts, and $\gamma_{sv}$ is the surface free energy of the substrate.

$$\cos\theta = -1 + 2\sqrt{\frac{\gamma_{sv}}{\gamma_{lv}}}\exp\left[-\beta\left(\gamma_{lv} - \gamma_{sv}\right)\right] \tag{12}$$

So, the $\gamma_{sv}$ values of MgO and $TiO_2$ substrates are 926 and 805 mJ/m², respectively. This also confirms that the large equilibrium contact angle corresponds to high surface energy. Thus, it can be concluded the Al-8Si/MgO system has better non-wetting properties than Al-8Si/$TO_2$ system. In addition, Ti is a reactive element for Al-8Si/$TiO_2$ system, which can improve the interface wettability by decreasing liquid/solid interfacial free energy[25]. Also, the existence of Ti can promote the interface reaction and increase the thickness of interface reaction layer (Fig. 5). In contrast, the interface reaction accelerates the exchange of substances near the triphase line and promotes the migration of the triphase line, resulting in a lower ECA of $TiO_2$/Al-8Si system. This is also another factor leading to the good wettability of Al-8Si/$TiO_2$ compared with Al-8Si/MgO.

## 3 Conclusions

1) Interface microstructure of Al-8Si/stainless steel is composed of Fe(Al, Si)$_3$, $Al_{7.2}Fe_{1.8}Si$ and $Fe_2Al_5$ phase, while that of Al-8Si/MgO and Al-8Si/$TiO_2$ systems consists mainly of $Al_2O_3$ phase.

2) The wettability results of three systems indicate that the Al-8Si/MgO system exhibits a better non-wettability compared with the Al-8Si/stainless steel and Al-8Si/$TiO_2$ systems, whose equilibrium contact angle (124°) is higher than that of the stainless steel (29°) and $TiO_2$ (96°) substrate.

3) The wettability differences of the three systems are mainly related to the roughness and properties of interface products. The interface roughness tests indicate that the Al-8Si/MgO system has the largest roughness of 1.46 μm compared with Al-8Si/stainless steel and Al-8Si/$TiO_2$ systems. The larger interface roughness increases the surface free energy of interface reaction layer and improves the non-wetting property of the system.

## References


1 Guan R G, Zhao Z Y, Chao R Z *et al. Transactions of Nonferrous Metals Society of China*[J], 2012, 22(12): 2871

2 Ueki M, Naka M, Okamoto I. *Journal of Materials Science Letters*[J], 1986, 5(12): 1261

3 Shen P, Fujii H, Matsumoto T *et al. Acta Materialia*[J], 2004, 52(4): 887

4 Budka W J, Stank K, Nowak R *et al. Journal of Materials Science*[J], 2016, 51(4): 1692

5 Cong X S, Shen P, Wang Y *et al. Applied Surface Science*[J], 2014, 317: 140

6 Ksiazek M, Sobczak N, Mikulowskl B *et al. Materials Science and Engineering A: Structural Materials*[J], 2002, 324(1): 162

7 Shen P, Fujii H, Nogi K. *Acta Materialia*[J], 2005, 54(6): 1559

8 Young T. *Philosophical Transactions of the Royal Society of London*[J], 1805, 95: 65

9 Yang N N, Gu Y, Cao K Z. *Superlattices and Microstructures*[J], 2015, 82: 158

10 An Q, Cong X S, Shen P *et al. Journal of Alloys and Compounds*[J], 2019, 784: 1212

11 Avraham S, Kaplan W D. *Journal of Materials Science*[J], 2005, 40(5): 1093

12 Lin Q L, Cao R, Jin P *et al. Surface and Coatings Technology*[J], 2016, 302: 166

13 Lin Q L, Li F X, Jin P *et al. Vacuum*[J], 2017, 145: 95

14 Liu Z Y, Yang J, Li Y L *et al. Applied Surface Science*[J], 2020, 520: 146 316

15 Lin S B, Song J L, Yang C L *et al. Acta Metallurgica Sinica*[J], 2009, 45(10): 1211

16 Barin I. *Thermochemical Data of Pure Substances*[M]. New York: VCH, 1995

17 Yang L, Xia M X, Babu N H *et al. Materials Transactions*[J], 2015, 56(3): 277

18 Nowak R, Sobczak N, Sienicki E *et al. Solid State Phenomena*[J], 2011, 173: 1278

19 Hu S P, Chen Z B, Lei Y Z *et al. Rare Metal Materials and Engineering*[J], 2019, 48(3): 701

20 Zhang J X, Xue S B, Xue P *et al. Rare Metal Materials and Engineering*[J], 2017, 46(7): 1900

21 Lin Q L, Wang L, Sui R. *Acta Materialia*[J], 2021, 203(15): 116 488

22 Jin P, Zhong W Q, Li F X *et al. Materials Review*[J], 2017, 31(9): 59

23 Qi Z, Liao L, Wang R Y *et al. Transactions of Nonferrous Metals Society of China*[J], 2021, 31(8): 2511

24 Li D, Neumann A W. *Journal of Colloid and Interface Science*[J], 1992, 148(1): 190

25 Sui R, Ju C Y, Zhong W Q *et al. Journal of Alloys and Compounds*[J], 2018, 739: 61

# 1173 K下Al-8Si二元合金对MgO、$TiO_2$和不锈钢的润湿作用

毕广利[1,2]，齐珈晨[1,2]，姜　静[1,2]，林巧力[1,2]，李元东[1,2]，陈体军[1,2]，马　颖[1,2]，管仁国[3]

(1. 兰州理工大学 省部共建有色金属先进加工与再利用国家重点实验室，甘肃 兰州 730050)

(2. 兰州理工大学 材料科学与工程学院，兰州 730050)

(3. 大连交通大学 材料科学与工程学院，大连 116028)

**摘　要**：采用改良座滴法对Al-8Si/不锈钢、Al-8Si/MgO和Al-8Si/$TiO_2$体系的润湿性和界面组织进行了研究。从热力学角度讨论了3个体系界面反应产物的形成。结果表明，Al-8Si/不锈钢的界面组织由$Fe(Al,Si)_3$、$Al_{7.2}Fe_{1.8}Si$和$Fe_2Al_5$相组成，而Al-8Si/MgO和Al-8Si/$TiO_2$体系的界面组织主要由不同形貌$Al_2O_3$相组成。3种体系的润湿性测试结果表明，Al-8Si熔体在MgO上具有较好的非润湿性能，其平衡润湿角为124°。3种体系润湿性的差异主要与界面产物的性质和粗糙度有关。界面粗糙度测试结果表明，Al-8Si/MgO体系界面粗糙度最大，为1.46 μm，主要原因是界面反应过程中Mg的蒸发破坏了界面反应层的形貌，此外Ti的存在促进了Al-8Si/$TiO_2$体系的界面反应，增加了界面反应层的厚度，降低了平衡润湿角。

**关键词**：Al-8Si合金；润湿性；2520不锈钢；$TiO_2$；MgO

---

作者简介：毕广利，男，1981年生，博士，教授，兰州理工大学省部共建有色金属先进加工与再利用国家重点实验室，甘肃 兰州 730050，电话：0731-2976378，E-mail：glbi@163.com